ACS APPLIED MATERIALS & INTERFACES

www.acsami.org

Research Article

Upcycling Microbial Cellulose Scraps into Nanowhiskers with Engineered Performance as Fillers in All-Cellulose Composites

Pamela T. S. Melo, Caio G. Otoni, Hernane S. Barud, Fauze A. Aouada, and Márcia R. de Moura*

Cite This: *ACS Appl. Mater. Interfaces* 2020, 12, 46661−46666

Read Online

ACCESS | Metrics & More | Article Recommendations

ABSTRACT: Cellulose is everywhere and renovates in nature continuously and rapidly, while petroleum does not. Unlike the latter, cellulose biodegrades and may represent a carbon sink. Inspired by the multiscale architecture of cellulose, we report on all-cellulose composites comprising cellulose ether as a matrix and highly pure bacterial cellulose nanocrystals (BCNCs) as fillers. Optimum performance as a packaging material was achieved by engineering BCNC surface chemistry as well as the filler-in-matrix dispersion, targeting the replacement of unsustainable, fossil-derived plastics intended for single-use applications. Cost could pose a hurdle, eliminated through the valorization of underutilized scraps from industrial operations, which is also in line with the circular bioeconomy in terms of the integral use of biomass. As far as performance, the optically transparent hydroxypropyl methylcellulose (HPMC) films presented improved tensile strength (from 61 ± 6 to 86 ± 9 MPa) and Young's modulus (from 1.5 ± 0.2 to 2.7 ± 0.4 GPa) while reduced elongation at break (from 15 ± 2 to 12 ± 2%) and water vapor permeability (from 0.40 ± 0.02 to 0.31 ± 0.01 g mm h^{-1} m^{-2} kPa^{-1}) when filled with only 5 wt % of (120 ± 31) nm long, (13 ± 3) nm wide, 88% crystalline BCNC. This dual, win−win effect of BCNCs on the mechanical and barrier properties of HPMC films was enabled by a suitable dispersion state, achieved *via* high-energy mixing, and quenched by casting. This study adds to the current literature on all-cellulose composites and helps pave the route for the technical and economical feasibilities of replacing non-renewable, non-biodegradable plastics in short-term applications by materials that are both renewable and biodegradable, that are also produced through green protocols and isolated from surplus biomass, and that still perform similarly or even better.

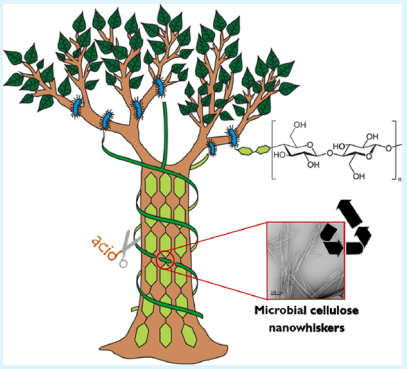

KEYWORDS: *bionanocomposite, waste valorization, nanocellulose, bacterial cellulose, biocellulose, cellulose nanocrystals*

INTRODUCTION

As plastics continuously increase in importance within virtually all spheres of today's society, non-renewable sources of monomers are gradually exhausted at the expense of the endless accumulation of non-biodegradable parts and comminuted microplastics in the environment.[1,2] Sustainability is therefore chased more and more, and a means of achieving so in the context of plastics is by shifting toward biopolymers, that is, bio-based and/or biodegradable polymers.[3] The indiscriminate exploitation of rapidly renewable resources for plastic production is not sustainable either,[4] highlighting waste valorization as a relevant strategy to achieve integral use of biomass. In this context, reprocessing residues from processed goods denotes a promising approach to help mitigate the human footprint on the environment, particularly when dealing with plastics designed for short-term applications, for example, single-use packaging.[5]

Cellulose is a fascinating polysaccharide that is both naturally occurring and biodegradable. It is highly versatile and can be used either as a continuous matrix or in its colloidal form—the so-called nanocelluloses, that is, cellulose nanofibrils (CNFs) or cellulose nanocrystals (CNCs)—to hierarchically assemble sustainable, yet multifunctional materials.[6] In order to parallel traditional materials in terms of performance, all-cellulose (nano)composites films,[7−11] filaments,[12] and beads[13] have been extensively reported lately. Higher plants have been by far the major source of (nano)celluloses, which can also be bottom-up extruded by some strains of bacteria, termed as bacterial cellulose (BC), microbial cellulose, or biocellulose. While the conventional top-down isolation from plants leads to lignocellulosics, that is, a complex mixture of cellulose, hemicellulose, lignin, and extractives, which may be beneficial in some situations, BC is devoid of any of these non-cellulosic substances.[14] This implies that the recalcitrance of the latter biomass is lower and that

Received: July 8, 2020
Accepted: September 16, 2020
Published: September 16, 2020

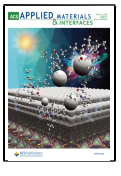

https://dx.doi.org/10.1021/acsami.0c12392
ACS Appl. Mater. Interfaces 2020, 12, 46661−46666

nanocellulose isolation is facilitated when compared to the botanical route. In addition to being purer, bacterial nanocelluloses feature larger specific surface areas than their vegetal counterparts due to the long subfibrils of the formers.[15]

Bacterial CNCs (BCNCs) are among the nanosized entities that can be isolated from BC and whose benefits when added into polymer-based nanocomposites as fillers for mechanical reinforcement purposes have been depicted. These nanostructures merge inherent characteristics of their precursors: the purity of BC, the high specific surface area and aspect ratio of rod-like nanostructures, and the high crystallinity and stiffness of CNCs. Depending on the isolation route, charged groups may be introduced on the surface of BCNCs, providing them with improved colloidal stability arising from electrostatic repulsion.[16] This is beneficial for composites because filler-in-matrix dispersion is a key factor enabling optimum transfer of mechanical stress, while filler aggregation may give rise to stress raisers.[7,17] Using a cellulosic matrix as a binder for BCNCs (*i.e.*, all-cellulose composites) is an interesting approach because of the chemical compatibility among the phases,[18] leading to proper matrix/filler interactions and benefited mechanical and barrier properties, to mention a few. Hydroxypropyl methylcellulose (HPMC) is a cellulose ether that serves as a proper matrix for such materials because of its good film-forming ability and nonionic nature,[7] avoiding matrix/filler repulsion in case both are negatively charged or prompt matrix/filler complexation if these phases are unlikely charged.

Within this agenda, we herein used a biorefinery approach to upcycle the scraps resulting from the commercial shaping of BC sheets into wound dressings. The main objective was to isolate negatively charged BCNCs from the low-value-added scraps and promote their proper dispersion as fillers within a cellulose ether matrix into all-cellulose nanocomposite films. Improved performance as far as flexible packaging, a major jeopardizer of sustainability in the context of plastic littering, was also targeted by taking mechanical and water barrier properties as response variables for optimization purposes. This contribution adds to the existing literature on BCNC-containing systems *via* its waste valorization and all-cellulose material perspectives.

EXPERIMENTAL SECTION

Materials. HPMC Methocel K4M (CAS no. 9004-65-3; The Dow Chemical Company, Brazil; average methoxyl/hydroxypropyl ratio: 2.26), sodium chloride (CAS no. 7440-23-5; Sigma-Aldrich, USA), and sulfuric acid (CAS no. 7664-93-9; Êxodo Científica, Brazil) were used without further purification. BC scraps resulting from cutting operations of biocellulose films for commercial production of wound dressings were kindly provided by Nexfill (Brazil) and used as a source of BCNCs. Deionized Milli-Q water (Millipore Corp., USA; resistivity of 18.2 MΩ) was used in all investigations.

Isolation of BCNCs. BCNCs were isolated from the BC scraps *via* sulfuric acid hydrolysis, as described elsewhere.[19] Briefly, the scraps were milled into powder and allowed to react with a 64 vol % sulfuric acid solution in water (17.5 mL of solution per g of powder) under mechanical stirring at 500 rpm and 50 °C for 50 min. The BCNC suspension was washed with ice-cold water (1:10 volume ratio) and centrifuged at 6000 rpm for 10 min to remove excess sulfuric acid. The sediment was dialyzed against ultrapure water through 14 kDa cutoff membranes until neutral pH was obtained.

Transmission Electron Microscopy. The BCNC suspensions were diluted to 0.01 wt % in ultrapure water, properly dispersed by alternating cycles of vortexing and ultrasound bath, deposited onto Ultrathin Holey Carbon Copper 400 mesh grids, dyed by a 2% uranyl acetate solution, and allowed to dry. The grids were imaged on a JEM-1400 PLUS electron microscope operating in a transmission mode (JEOL Inc., USA).

Apparent Zeta Potential. The apparent zeta potential of 2 wt % BCNC suspensions, added by 5 mM NaCl,[20] was determined through electrophoretic mobility measurements on a Zetasizer Nano ZS (Malvern Instruments, UK) at room temperature. Measurements were performed in triplicate.

Film Formation. HPMC-only films and HPMC-based composites containing 2.5 or 5 wt % (dry basis) of BCNCs were produced by solvent casting. Film-forming dispersions (FFDs) were obtained by mixing (i) 78.4 g of water, 1.6 g of HPMC, and 0.04 or 0.08 g of BCNCs at 10,000 rpm for 2 min using an Ultra-Turrax T18 (IKA, Germany) or (ii) at 500 rpm for 30 min on a magnetic stirrer. The FFD was deposited onto a 15 cm × 20 cm polyethylene substrate and allowed to dry for 24 h at 25 ± 5 °C. Dried films were equilibrated at 50% relative humidity (RH) for at least 48 h before testing.

X-ray Diffraction. X-ray diffraction (XRD) of BCNCs, HPMC-only films, and BCNC-containing HPMC films, mounted onto a glass sample holder, were acquired on a XRD-6000 diffractometer (Shimadzu, Japan) with Cu Kα radiation (λ = 1.54056 Å) using a pitch of 0.01° and Bragg angles (2θ) varying from 4 to 60° at 1° min^{-1}. The Segal crystallinity index of BCNCs was determined by normalizing the relative intensity assigned to the crystalline region (intensity at 22.7° minus that in the amorphous region at *ca.* 18°) by the intensity at 22.7°.[21]

Light Transmittance. The light transmittance through the HPMC films and their nanocomposites was measured on a UV-2600 spectrophotometer (Shimadzu, Japan) equipped with an integrating sphere accessory. Rectangular films with dimensions of 45 mm × 30 mm (length × width) were inserted in the sample holder and had their transmittance profiles acquired at wavelengths varying from 200 to 1000 nm.[22]

Water Vapor Permeability. The water vapor permeability (WVP) of the films was measured in 15.5 cm diameter circles fixed in a standard cell containing 6 mL of distilled water. Thereafter, samples were stored in a cabinet at 25 °C with moisture control. Six measurement weights of the cells were realized on an analytical balance over a total period of 25 h (at the begin test and after 1, 2, 23, 24, and 25 h). The test was performed in triplicate for each film. Film thickness was measured using a digital micrometer (Mitutoyo, Japan) with 0.001 mm resolution and 0−25 mm of capacity. Measurements were realized at five random points along each film sample.

Mechanical Properties. The nanocomposites were characterized as to their mechanical properties—tensile stress (TS) at break, elongation at break (EB), and Young's modulus (YM)—through uniaxial tensile assays on a universal testing machine (model 3369, Instron Corp., Canton-MA, USA), operating with a 100 N load cell and stretching the specimens at 10 mm min. The reported results are the average of at least six specimens per treatment. The tensile assays were carried out at 30 °C and 50% RH.

Scanning Electron Microscopy. Film morphology was analyzed through scanning electron microscopy (SEM) on an EVO LS15 microscope (Zeiss, Germany). The samples were cryo-fractured in liquid nitrogen, mounted onto aluminum stubs using a double-sided carbon tape (Ted Pella Inc., Redding, USA), and coated with a thin gold/palladium alloy layer through sputtering on a Quorum Q150T E. Magnifications of 10,000× and an acceleration voltage of 10 kV were used.

RESULTS AND DISCUSSION

Motivation for Upcycling Microbial Cellulose Scraps. As illustrated in Figure 1, Gram-negative acetic acid bacteria such as *Gluconacetobacter xylinus* use low-molecular weight carbon sources to produce BC sheets with a range of commercial applications, among which the biomedical field outstands.[23] After purification, drying, and shaping, these BC sheets serve as wound dressings commercially (red route). The cutting step generates a large amount of scraps that do not

https://dx.doi.org/10.1021/acsami.0c12392
ACS Appl. Mater. Interfaces 2020, 12, 46661−46666

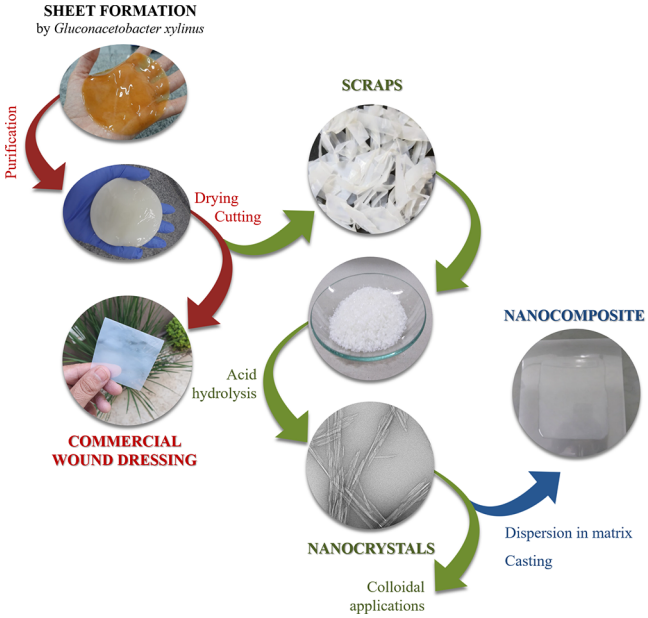

Figure 1. Commercial use of microbial cellulose membranes as wound dressings (red workflow) and isolation of CNCs from cutting-derived residues for application in colloidal systems (green workflow) or as fillers in nanocomposite films (blue arrow).

follow the commercial route and end up being discarded or used in low-value-added applications. To join efforts toward the maximum exploitation of biomass, and to increase the competitiveness of BCNCs in terms of production costs, only the scraps were used herein as a source of BCNCs. This biorefinery approach also adds value to the BC business, which then generates less waste and features broadened range of applications. As depicted below, the BC scraps were submitted to both chemical and mechanical treatments at optimized conditions, resulting in versatile BCNCs that can be either used as biocolloids in suspension (green route) or dried into solid-state materials, including polymer-based nanocomposites (blue route). The red−green−blue track was followed in this contribution, culminating in BCNC-reinforced all-cellulose composites.

Bacterial CNCs. Transmission electron microscopy (TEM) revealed stiff, spindle-like BCNCs featuring an average length of 120 ± 31 nm (Figure 2C) and width of 13 ± 3 nm (Figure 2D) as well as aspect (length-to-width) ratio of 10 ± 3, value which falls within the typical range of CNCs, that is, 5−30.[20] Similar dimensions have been reported for CNCs of the same origin. The BCNC was suspended in water into a colloidally stable system (Figure 2b). While CNF suspensions are widely known to present steric stability arising from the highly entangled state, CNC suspensions are often associated to electrostatic stability due to the presence of electrically charged or ionizable surface groups, depending on the isolation route. The herein isolated BCNC presented a zeta potential of −45 ± 4 mV, resulting from replacement of hydroxyl groups (protonated at pH < 12) by sulfate half-ester groups upon hydrolysis with sulfuric acid.[20,24] As a matter of fact, absolute zeta potential values higher than 20 mV have been attributed to colloidal stability due to electrostatic repulsion among likely charged particles.[25]

XRD (Figure 3) confirms the high crystallinity (Segal index: 88%; similar to other reports)[26] of the BCNC. It also evidences that the crystalline structure that is the typical characteristic of type-I cellulose remained unscathed after acid hydrolysis. Specifically, the three sharp peaks at *ca.* 14.6, 16.9, and 22.7° are assigned, respectively, to the (10), (110), and (200) planes that are characteristic of the Iα (triclinic) allomorph, which in turn prevails in BC.[19,27]

All-Cellulose Composite Films. The isolated BCNCs were added at different contents to HPMC film-forming

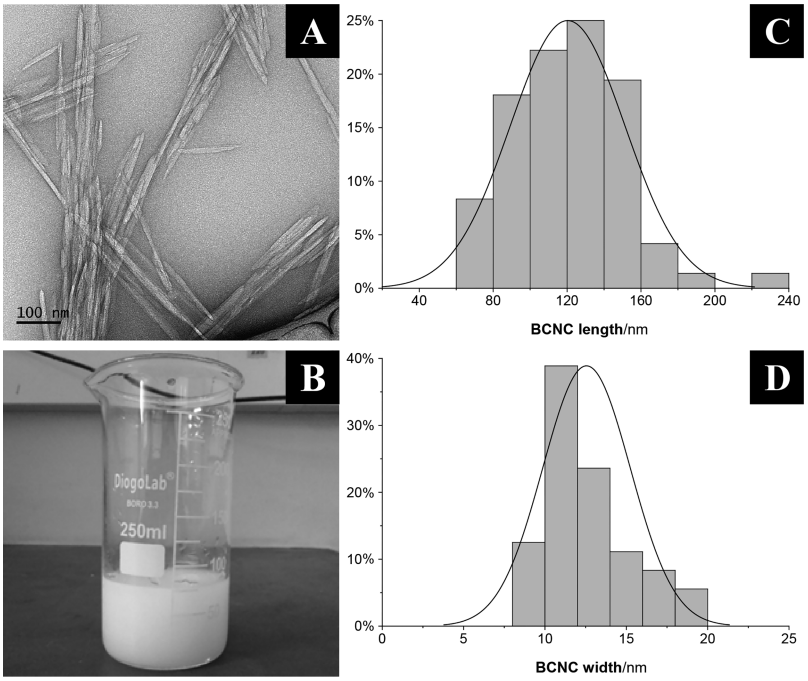

Figure 2. Representative transmission electron micrograph (A) and digital photograph (B) of an aqueous suspension of BCNCs. Distributions (normal distributions) of length (C) and width (D) of BCNCs. *Y*-axes: normalized particle counts (%; n = 73).

https://dx.doi.org/10.1021/acsami.0c12392
ACS Appl. Mater. Interfaces 2020, 12, 46661−46666

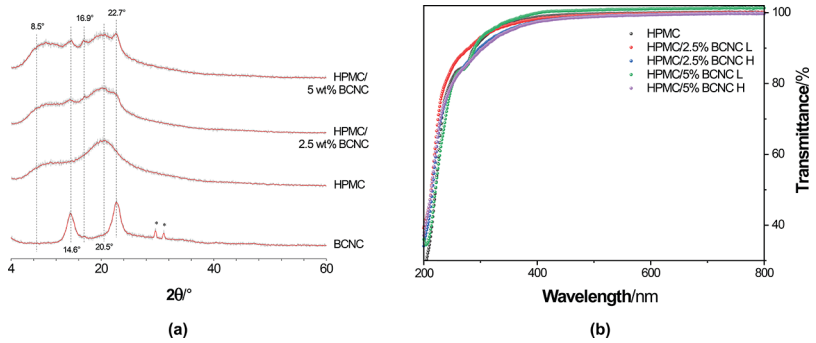

Figure 3. X-ray diffractograms (a) and optical transmittances (b) of HPMC films filled with 0−5 wt % (dry basis) of BCNCs. In (a), *y*-axis indicates intensity (a.u.) and peaks marked with * are assigned to the sample holder. In (b), L and H indicate low- and high-energy mixing, respectively.

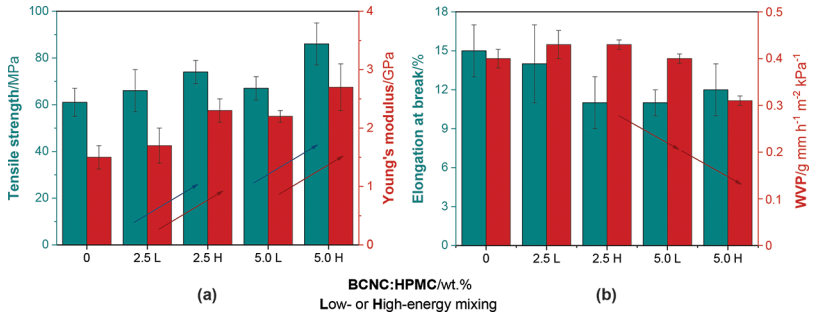

Figure 4. Mechanical properties [(a,b)—left *y*-axis] and WVP [(b)—right *y*-axis] of films from HPMC filled with 0−5 wt % (dry basis) of BCNCs *via* either low- or high-energy (L or H, respectively) mixing protocols.

formulations and solvent cast into all-cellulose composite films, all of which were macroscopically continuous (*i.e.*, devoid of macroscopic flaws), homogeneous (*i.e.*, lacking poorly dispersed domains and texture/colors gradients), and pliable (*i.e.*, flexible enough to manipulate and peel off from the casting surface without impaired integrity). All films showed the same ($p > 0.05$, according to analysis of variance—ANOVA) thickness, with an average value of 28 ± 2 μm. The XRD patterns of the BCNC-added film (Figure 3a) evidence the crystal structure of the BCNC, which was absent in the HPMC-only sample but increase in intensity as the BCNC content is increased from 2.5 to 5 wt %. The HPMC film itself presented rather wide peaks centered at *ca.* 8.5 (101) and 20.5° (002), evidencing its predominantly amorphous but semi-crystalline structure.[28] As far as optical properties are concerned, all films were optically transparent, as indicated by transmittances close to 100% at 600 nm (Figure 3b)—mind that thickness was the same regardless of composition. This corroborates the proper dispersion of BCNCs within the HPMC matrix as nanoparticle aggregates would otherwise impair light transmittance. The effects of BCNC addition on the mechanical and water barrier properties of HPMC films are depicted in Figure 4.

Figure 4a demonstrates the mechanical reinforcement role played by BCNCs in HPMC films, effects which have been widely reported for nanocelluloses when added to a plethora of biopolymer-based films.[29] Additionally, one may notice that this effect took place herein in a composition- and processing-dependent fashion. Regardless of the mixing protocol, 5 wt % of the BCNC was successful in stiffening HPMC-only films, as indicated by the increased Young's moduli. Even 2.5 wt % was enough to significantly ($p < 0.05$, according to ANOVA followed by Tukey's test) increase the rigidity of the HPMC film but only when the BCNC was dispersed into the film-forming formulation through a high-energy protocol. This is a clear outcome of the filler-in-matrix state of dispersion, which must be sufficiently high to prevent particle aggregation that is known to create stress raisers as well as to decrease the specific filler/matrix interfacial area, impairing the load transfer efficiency.[7] Comparably, Salari et al.[30] found CNCs to reinforce chitosan films when the particles were homogeneously dispersed within the nanocomposite, favoring filler/matrix interactions and the effective matrix-to-filler load transfer. A similar effect was observed on the tensile strength of HPMC-only films, which became more resistant ($p < 0.05$) upon BCNC addition followed by a high-energy procedure, regardless of the BCNC-to-HPMC ratio. On the other hand, the low-energy mixing was ineffective ($p > 0.05$) in increasing the tensile strength of HPMC films, regardless of the BCNC content.

While increasing the tensile strength and YM of HPMC-only films to 41 and 80%, respectively, adding 5 wt % of the BCNC through a high-energy mixing process did not affect ($p > 0.05$) the EB (Figure 4b), although some of the treatments did reduce film extensibility, as reported elsewhere for similar systems.[7,29] The aforementioned treatment also lessened ($p < 0.05$) the WVP of HPMC-only films in 22.5%, whereas none of the others affected ($p > 0.05$) the WVP of pristine HPMC films. Because low WVP values are typical of good barriers to moisture, one may conclude that HPMC films may represent a better barrier material when filled with the BCNC, though depending on the filler content and mixing protocol. With both the matrix and the filler being hydrophilic components, the improved water barrier character is attributed to the enhanced state of BCNC-in-HPMC dispersion upon high-energy mixing as well as to the formation of a hydrogen bonding network

https://dx.doi.org/10.1021/acsami.0c12392
ACS Appl. Mater. Interfaces 2020, 12, 46661−46666

between the hydroxyl groups in HPMC and BCNC, improving film cohesiveness. As a matter of fact, the SEM images of films prepared *via* high-intensity mixing (Figure 5) demonstrate

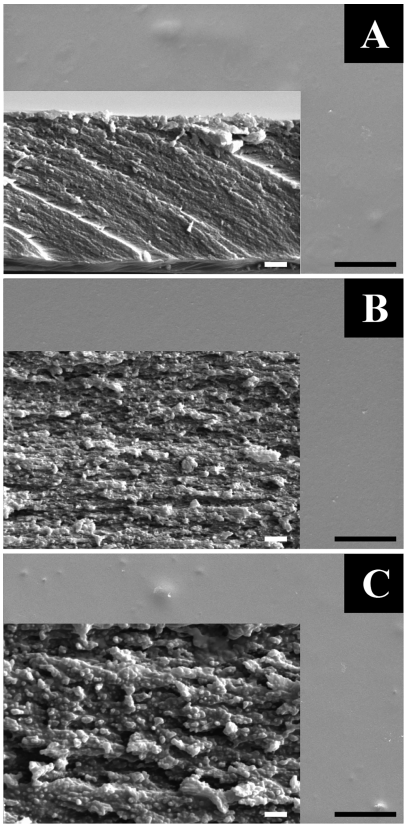

Figure 5. Surface (large images; black scale bars: 20 μm) and cross-sectional (insets; white scale bar: 2 μm) scanning electron micrographs of HPMC films filled with 0 (control; A), 2.5 (B), and 5 (C) wt % (dry basis) of BCNCs.

homogeneous surfaces in all films as well as evenly distributed fillers within the cross-sections of the BCNC-containing HPMC matrices, regardless of the BCNC load. Additionally, as far as WVP, the highly crystalline BCNC acts as a barrier to water molecules, making the diffusive path more tortuous and, as a result, longer.[31,32] In line, Ma et al.[33] highlighted filler aggregation as a factor shortening the pathway for water vapor to diffuse through a biopolymer film, increasing its WVP.

CONCLUSIONS

In summary, optically transparent HPMC-based, BCNC-reinforced all-cellulose composite films were produced *via* green, straightforward protocols and exhibited suitable properties for packaging applications. Engineering the surface chemistry of BCNCs and their state of dispersion within the HPMC matrix, despite the low load, allowed the barrier to moisture and the mechanical resistance and stiffness to be boosted by 20+, 40+, and 80%, respectively, while extensibility was only decreased by 20%. It is important to stress out that the BCNCs were isolated from surplus biomass, complying with the trends toward biorefineries and circular bioeconomy as well as potentially reducing production costs to compare with conventional plastics not only in terms of performance but also production costs. This outcome has clear implications in the recent efforts of the scientific community to make the replacement of non-renewable, non-biodegradable plastics by all-cellulose composites feasible both technically and economically, in particular for short-term applications such as packaging materials.

AUTHOR INFORMATION

Corresponding Author

Márcia R. de Moura − *Grupo de Compósitos e Nanocompósitos Híbridos (GCNH), Department of Physics and Chemistry, Ilha Solteira School of Engineering, São Paulo State University (UNESP), 15385-000 Ilha Solteira, São Paulo, Brazil;* orcid.org/0000-0002-2534-5553; Phone: +55-18-3743-1961; Email: marcia.aouada@unesp.br

Authors

Pamela T. S. Melo − *Grupo de Compósitos e Nanocompósitos Híbridos (GCNH), Department of Physics and Chemistry, Ilha Solteira School of Engineering, São Paulo State University (UNESP), 15385-000 Ilha Solteira, São Paulo, Brazil*

Caio G. Otoni − *Institute of Chemistry, University of Campinas (UNICAMP), 13083-970 Campinas, São Paulo, Brazil;* orcid.org/0000-0001-6734-7381

Hernane S. Barud − *Laboratory of Biopolymers and Biomaterials (BioPolMat), University of Araraquara (UNIARA), 14801-340 Araraquara, São Paulo, Brazil;* orcid.org/0000-0001-9081-2413

Fauze A. Aouada − *Grupo de Compósitos e Nanocompósitos Híbridos (GCNH), Department of Physics and Chemistry, Ilha Solteira School of Engineering, São Paulo State University (UNESP), 15385-000 Ilha Solteira, São Paulo, Brazil*

Complete contact information is available at: https://pubs.acs.org/10.1021/acsami.0c12392

Notes

The authors declare no competing financial interest.

ACKNOWLEDGMENTS

The authors are thankful to the TEM facilities at the Brazilian Nanotechnology National Laboratory (LNNano)/Brazilian Center for Research in Energy and Materials (CNPEM) and the technical support by Dr. M. A. Farias. F. A. Aouada thanks the Brazilian National Council for Scientific and Technological Development (CNPq; grant no. 312414/2018-8). M. R. de Moura thanks the São Paulo Research Foundation (FAPESP) (grant nos. 2019/06170-1 and 2013/07296-2 CEPID) and CNPq (grant no. 312530/2018-8). H. S. Barud thanks CNPq (grant no. 407822/2018-6; INCT-INFO), FAPESP (grant nos. 2018/25512-8 and 2013/07276-1 CEPID), and TA Instruments Brasil. The donation of microbial cellulose scraps by Seven Biotecnologia/Nexfill (Brazil) is highly appreciated. The Department of Physics and Chemistry of the São Paulo State University (UNESP) and the PROPG are acknowledged for the financial support. This study was financed in part by the Coordenação de Aperfeiçoamento de Pessoal de Nível Superior − Brasil (CAPES; Finance Code 001.2019).

REFERENCES

(1) Geyer, R.; Jambeck, J. R.; Law, K. L. Production, Use, and Fate of All Plastics Ever Made. *Sci. Adv.* **2017**, *3*, No. e1700782.

(2) Cozar, A.; Echevarria, F.; Gonzalez-Gordillo, J. I.; Irigoien, X.; Ubeda, B.; Hernandez-Leon, S.; Palma, A. T.; Navarro, S.; Garcia-de-Lomas, J.; Ruiz, A.; et al. Plastic Debris in the Open Ocean. *Proc. Natl. Acad. Sci. U.S.A.* **2014**, *111*, 10239−10244.

(3) Nunes, J. C.; Melo, P. T. S.; Lorevice, M. V.; Aouada, F. A.; de Moura, M. R. Effect of green tea extract on gelatin-based films incorporated with lemon essential oil. *J. Food Sci. Technol.* **2020**, DOI: 10.1007/s13197-020-04469-4.
(4) Gerngross, T. U.; Slater, S. C. How Green Are Green Plastics? *Sci. Am.* **2000**, *283*, 36−41.
(5) Zheng, J.; Suh, S. Strategies to Reduce the Global Carbon Footprint of Plastics. *Nat. Clim. Change* **2019**, *9*, 374−378.
(6) Kontturi, E.; Laaksonen, P.; Linder, M. B.; Nonappa; Gröschel, A. H.; Rojas, O. J.; Ikkala, O. Advanced Materials through Assembly of Nanocelluloses. *Adv. Mater.* **2018**, *30*, 1703779.
(7) Otoni, C. G.; Carvalho, A. S.; Cardoso, M. V. C.; Bernardinelli, O. D.; Lorevice, M. V.; Colnago, L. A.; Loh, W.; Mattoso, L. H. C. High-Pressure Microfluidization as a Green Tool for Optimizing the Mechanical Performance of All-Cellulose Composites. *ACS Sustainable Chem. Eng.* **2018**, *6*, 12727−12735.
(8) Khakalo, A.; Tanaka, A.; Korpela, A.; Hauru, L. K. J.; Orelma, H. All-Wood Composite Material by Partial Fiber Surface Dissolution with an Ionic Liquid. *ACS Sustainable Chem. Eng.* **2019**, *7*, 3195−3202.
(9) Hu, W.; Chen, G.; Liu, Y.; Liu, Y.; Li, B.; Fang, Z. Transparent and Hazy All-Cellulose Composite Films with Superior Mechanical Properties. *ACS Sustainable Chem. Eng.* **2018**, *6*, 6974−6980.
(10) Gustavsson, L. H.; Adolfsson, K. H.; Hakkarainen, M. Thermoplastic "All-Cellulose" Composites with Covalently Attached Carbonized Cellulose. *Biomacromolecules* **2020**, *21*, 1752−1761.
(11) Labidi, K.; Korhonen, O.; Zrida, M.; Hamzaoui, A. H.; Budtova, T. All-Cellulose Composites from Alfa and Wood Fibers. *Ind. Crops Prod.* **2019**, *127*, 135−141.
(12) Qiu, C.; Zhu, K.; Yang, W.; Wang, Y.; Zhang, L.; Chen, F.; Fu, Q. Super Strong All-Cellulose Composite Filaments by Combination of Inducing Nanofiber Formation and Adding Nanofibrillated Cellulose. *Biomacromolecules* **2018**, *19*, 4386−4395.
(13) Mystek, K.; Reid, M. S.; Larsson, P. A.; WÅgberg, L. In Situ Modification of Regenerated Cellulose Beads: Creating All-Cellulose Composites. *Ind. Eng. Chem. Res.* **2020**, *59*, 2968−2976.
(14) Klemm, D.; Cranston, E. D.; Fischer, D.; Gama, M.; Kedzior, S. A.; Kralisch, D.; Kramer, F.; Kondo, T.; Lindström, T.; Nietzsche, S.; et al. Nanocellulose as a Natural Source for Groundbreaking Applications in Materials Science: Today's State. *Mater. Today* **2018**, *21*, 720−748.
(15) Klemm, D.; Kramer, F.; Moritz, S.; Lindström, T.; Ankerfors, M.; Gray, D.; Dorris, A. Nanocelluloses: A New Family of Nature-Based Materials. *Angew. Chem., Int. Ed.* **2011**, *50*, 5438−5466.
(16) Habibi, Y.; Lucia, L. A.; Rojas, O. J. Cellulose Nanocrystals: Chemistry, Self-Assembly, and Applications. *Chem. Rev.* **2010**, *110*, 3479−3500.
(17) Mohanty, A. K.; Vivekanandhan, S.; Pin, J.-M.; Misra, M. Composites from Renewable and Sustainable Resources: Challenges and Innovations. *Science* **2018**, *362*, 536−542.
(18) Li, J.; Nawaz, H.; Wu, J.; Zhang, J.; Wan, J.; Mi, Q.; Yu, J.; Zhang, J. All-Cellulose Composites Based on the Self-Reinforced Effect. *Compos. Commun.* **2018**, *9*, 42−53.
(19) Lima, L. R.; Santos, D. B.; Santos, M. V.; Barud, H. S.; Henrique, M. A.; Pasquini, D.; Pecoraro, E.; Ribeiro, S. J. L. Cellulose Nanocrystals from Bacterial Cellulose. *Quim. Nova* **2015**, *38*, 1140.
(20) Foster, E. J.; Moon, R. J.; Agarwal, U. P.; Bortner, M. J.; Bras, J.; Camarero-Espinosa, S.; Chan, K. J.; Clift, M. J. D.; Cranston, E. D.; Eichhorn, S. J.; et al. Current Characterization Methods for Cellulose Nanomaterials. *Chem. Soc. Rev.* **2018**, *47*, 2609−2679.
(21) Segal, L.; Creely, J. J.; Martin, A. E.; Conrad, C. M. An Empirical Method for Estimating the Degree of Crystallinity of Native Cellulose Using the X-Ray Diffractometer. *Text. Res. J.* **1959**, *29*, 786−794.
(22) Zhong, M.; Jang, M. Light Absorption Coefficient Measurement of SOA Using a UV−Visible Spectrometer Connected with an Integrating Sphere. *Atmos. Environ.* **2011**, *45*, 4263−4271.
(23) Ferreira, F. V.; Otoni, C. G.; De France, K. J.; Barud, H. S.; Lona, L. M. F.; Cranston, E. D.; Rojas, O. J. Porous Nanocellulose Gels and Foams: Breakthrough Status in the Development of Scaffolds for Tissue Engineering. *Mater. Today* **2020**, *37*, 126.
(24) El Achaby, M.; El Miri, N.; Hannache, H.; Gmouh, S.; Ben youcef, H.; Aboulkas, A. Production of Cellulose Nanocrystals from Vine Shoots and Their Use for the Development of Nanocomposite Materials. *Int. J. Biol. Macromol.* **2018**, *117*, 592−600.
(25) Bhattacharjee, S. DLS and Zeta Potential − What They Are and What They Are Not? *J. Controlled Release* **2016**, *235*, 337−351.
(26) Machado, R. T. A.; Gutierrez, J.; Tercjak, A.; Trovatti, E.; Uahib, F. G. M.; Moreno, G. d. P.; Nascimento, A. P.; Berreta, A. A.; Ribeiro, S. J. L.; Barud, H. S. Komagataeibacter Rhaeticus as an Alternative Bacteria for Cellulose Production. *Carbohydr. Polym.* **2016**, *152*, 841−849.
(27) Henrique, M. A.; Flauzino Neto, W. P.; Silvério, H. A.; Martins, D. F.; Gurgel, L. V. A.; Barud, H. d. S.; Morais, L. C. d.; Pasquini, D. Kinetic Study of the Thermal Decomposition of Cellulose Nanocrystals with Different Polymorphs, Cellulose I and II, Extracted from Different Sources and Using Different Types of Acids. *Ind. Crops Prod.* **2015**, *76*, 128−140.
(28) George, J.; Kumar, R.; Sajeevkumar, V. A.; Ramana, K. V.; Rajamanickam, R.; Abhishek, V.; Nadanasabapathy, S.; Siddaramaiah. Hybrid HPMC Nanocomposites Containing Bacterial Cellulose Nanocrystals and Silver Nanoparticles. *Carbohydr. Polym.* **2014**, *105*, 285−292.
(29) Kargarzadeh, H.; Huang, J.; Lin, N.; Ahmad, I.; Mariano, M.; Dufresne, A.; Thomas, S.; Gałęski, A. Recent Developments in Nanocellulose-Based Biodegradable Polymers, Thermoplastic Polymers, and Porous Nanocomposites. *Prog. Polym. Sci.* **2018**, *87*, 197−227.
(30) Salari, M.; Sowti Khiabani, M.; Rezaei Mokarram, R.; Ghanbarzadeh, B.; Samadi Kafil, H. Development and Evaluation of Chitosan Based Active Nanocomposite Films Containing Bacterial Cellulose Nanocrystals and Silver Nanoparticles. *Food Hydrocolloids* **2018**, *84*, 414−423.
(31) Azeredo, H. M. C.; Rosa, M. F.; Mattoso, L. H. C. Nanocellulose in Bio-Based Food Packaging Applications. *Ind. Crops Prod.* **2017**, *97*, 664−671.
(32) Azeredo, H. M. C. d. Nanocomposites for Food Packaging Applications. *Food Res. Int.* **2009**, *42*, 1240−1253.
(33) Ma, X.; Cheng, Y.; Qin, X.; Guo, T.; Deng, J.; Liu, X. Hydrophilic Modification of Cellulose Nanocrystals Improves the Physicochemical Properties of Cassava Starch-Based Nanocomposite Films. *LWT* **2017**, *86*, 318−326.

https://dx.doi.org/10.1021/acsami.0c12392
ACS Appl. Mater. Interfaces 2020, 12, 46661−46666